Validity of the center-center method for the syndesmotic fixation axis compared to the trans-syndesmotic axis

（足関節骨折に伴う遠位脛腓靱帯損傷に対する新たな整復固定方法の妥当性の検討）

千葉大学大学院医学薬学府先進予防医学共同専攻

（主任：佐粧孝久教授）

中嶋　啓文

INTRODUCTION

Tibiofibular syndesmosis injuries are involved with 10 to 45 percent of ankle fractures that require operative treatment.[16, 23] Malreduction of the syndesmoses is associated with decreased ankle function and an increased risk of ankle osteoarthritis.[12] Despite this, up to 50 percent of patients have been reported to experience a suboptimal reduction of the syndesmosis on postoperative computed tomography (CT) scans.[8, 14]

Forceps are commonly used for tibiofibular reduction during surgery. However, improper clamping in the axial plane, followed by misaligned screw or suture button insertion, can result in malreduction of the syndesmosis.[6, 7, 17, 25] Clinical and cadaveric studies have shown that clamping along the trans-syndesmotic (TS) axis, which is perpendicular to the distal tibiofibular joint, prevents iatrogenic malreduction.[6, 7, 10, 18, 20] However, determining the TS axis is challenging intraoperatively because the surface of the tibiofibular joint is not directly visible. Conventionally, it is recommended to insert the syndesmotic screw at a 20 to 30 degrees angle from the posterolateral to the anteromedial plane.[15] However, the anatomical evidence for this recommendation is unclear,[15] and it can lead to off-axis screw placement due to the anatomical variation of the syndesmosis among individuals.[1]

The center-center (CC) method is an intraoperative fluoroscopic technique used to determine the position of the syndesmotic clamp,[4] in which an internally rotated lateral view of the ankle is obtained in the fluoroscopic image so that the anteroposterior center of the fibula overlies that of the tibia. The forceps are used to clamp the syndesmosis along the axis that passes through the centers of the fibula and tibia (CC axis). Surgeons can apply this technique at different heights from the articular surface of the ankle.[11, 19]

Whether the CC axis corresponds to the TS axis remains unclear. One study showed that the CC axis was highly consistent with the line connecting the geometrical centroids of the fibula and tibia in the axial plane.[11] But the centroid axis is not anatomically based on the tibiofibular joint. To date, no studies have clarified whether clamping along the CC axis can minimize the risk of syndesmotic malreduction. Furthermore, the optimal height above the tibiotalar joint for the CC method has not been clarified. The directions of the TS and CC axes vary depending on the height of the tibial plafond.[11, 18]

This study aimed to measure the differences between the TS and CC axes and compare the differences when the CC method was applied at different heights from the ankle joint. Based on previous studies on the syndesmotic anatomy,[11, 13] we hypothesized that the TS axis would be externally rotated relative to the CC axis and that the differences between the two axes would be larger when the CC method was applied at a higher height compared to when it was applied at a lower height.

METHODS

Patients

This was a cross-sectional study using CT. The inclusion criteria were patients who underwent CT for the examination of foot and ankle diseases at our hospital from April 2017 to March 2022. The exclusion criteria were: patients with (1) ankle osteoarthritis with Tanaka-Takakura stage 2 or higher,[22] (2) ankle fracture or history of ankle fracture; (3) bone destruction due to a tumor or inflammatory disease; (4) apparent paralytic disease; (5) slice thickness of CT greater than 1 mm; (6) plantar flexion angle of the ankle larger than 20 degrees on the CT images;[24] and (7) age less than 18 years. The unaffected side was used when CT was performed on both ankles. This study was approved by the research ethics committee of our institute. The requirement for informed consent was waived because of the retrospective nature of the study.

Digitally reconstructed radiography

Patients underwent CT scanning of the foot and ankle at a 0.5-mm slice pitch (Aquilion 64, Toshiba Medical Systems Corporation, Otawara, Tochigi, Japan). During scanning, patients were placed in the supine position with the knee and ankle joints in a neutral position. Digitally reconstructed radiographs were created using the CT data and a commercial image reconstruction program (AquariusNet, TeraRecon, Foster City, CA, USA) linked to the electronic medical records. Firstly, the CT data were reconstructed into a three-dimensional image of the ankle (Figure 1A). Secondly, the three-dimensional CT was converted into a digitally reconstructed radiographic image resembling a plain radiograph by adjusting the window level (295 HU), window width (482 HU), and transparency (0.10) (Figure 1B). Finally, the operator was able to rotate the image in any direction in a three-dimensional virtual space on the computer screen, mimicking intraoperative fluoroscopy.

Center-center method

The digitally reconstructed radiographic ankle was aligned to visualize the talar dome lateral view, where the medial and lateral edges of the talar dome overlapped,[21] and the tibial longitudinal axis was aligned vertically (Figure 1B). Then, the operator internally rotated the ankle along the tibial longitudinal axis so that the anteroposterior centers of the fibula and tibia were superimposed at the ankle joint level using the CC method at a height of 0 mm from the tibial plafond (Figure 1C).[4] The center of the line connecting the anterior and posterior edges of each bone was determined using the length measurement function of the image reconstruction program. The program provided an axial CT image at a height of 0 mm (Figure 2A). When the operator rotated the digitally reconstructed radiographic image, the corresponding axial image also rotated, so the CC axis was always aligned horizontally in the image (Figure 2A).

Image measurements

The TS and CC axes were drawn on axial CT images (Figure 2A). The CC axis is defined as the line created by the CC method.[4, 11] The TS axis was a line perpendicular to the tangential line to the anterior and posterior notches of the fibular incisura,[7, 5, 18] which passes through the intersection between the CC axis and lateral edge of the fibula. The angle between the TS and CC axes was defined as the inter-axes angle. When the TS axis was externally rotated relative to the CC axis, the angle was expressed as a positive value. The distance between the intersectional points of the two axes and the medial tibial cortex was defined as the inter-axes distance (Figure 2B), with a positive value when the intersection of the TS axis was anterior to that of the CC axis. The angular measurements were performed with an increment of 0.1 degrees. The distance measurements were performed with an increment of 0.1 mm.

The same procedures, from the CC method using DRR to the image measurement, were repeated at different heights from the tibial plafond: 0, 10, and 20 mm. The heights were determined based on previous reports that assessed the TS and CC axes using CT. [11, 15, 18]

Syndesmotic anatomy

Rotation and depth of the fibular incisura were measured according to the previously reported methods using the CT images at 10 mm from the tibial plafond.[3] These anatomical variations were selected because they are associated with syndesmotic malreduction.[3, 5] Regarding the rotation, ankles were divided into anteverted (rotational angle of 8 degrees or higher) and retroverted (less than 8 degrees).[3] For the depth, ankles were divided into deep (incisura depth of 4 mm or higher) and shallow (less than 4 mm).[3]

Statistical analysis

Patient backgrounds and image measurements were presented as means and standard deviations because the data were normally distributed. To assess the overall association between the TS and CC axes, all image measurements, including inter-axes angles and distances at heights of 10, 20, and 30 mm, were pooled to calculate the mean values. One-way repeated-measures analysis of variance and post hoc Bonferroni tests were used to compare the image measurements at the three different heights. Additionally, angular differences between the CC axes at different heights and those between the TS axes were calculated.

To assess the intra-rater reliability of the image measurements, a senior orthopedic resident assessed 30 randomly selected images at a two-week interval. The two measurements were compared using the Bland-Altman analysis.[9] The mean difference, with a 95% confidence interval, and 95% limits of agreement were calculated. To assess the inter-rater reliability, a certified orthopedic surgeon evaluated the same 30 images, and the results were compared with those of the first evaluation by a senior resident. The Bland-Altman analysis was again used to compare the measurements of the two raters. The statistical significance level was set at a *P* value less than .05.

We calculated the sample size using the data from the first 20 patients. We estimated that the difference in the inter-axes angle at a height of 0 mm was 2 degrees, with an SD of 6.5 degrees between the population and sample means. Assuming a significance level of 5 percent and a power of

95 percent, the required sample size was 146.

RESULTS

Of the 237 patients screened, 150 were included in this analysis after excluding 87 (Figure 3). The patients had a mean age of 51 years, and the most common reasons for undergoing a CT examination were foot and ankle fractures and dislocations (n = 39), bone and soft tissue tumors (n = 33), and hallux rigidus (n = 20) (Table 1). Data from the unaffected side was used in 35 patients.

Overall, the TS axis was externally rotated relative to the CC axis, with a mean inter-axes angle of 8.5 degrees (standard deviation, 6.8 degrees) (Table 2). The inter-axes angle was 1.9 degrees at a height of 0 mm. The values were higher when the CC method was performed higher on the tibial plafond ($P < .001$), with post hoc tests showing significant differences among all heights (Table 2). Moreover, the intersection point of the TS axis with the medial tibial cortex was anterior to the intersection of the CC axis, with an inter-axes distance of 7.7 (standard deviation, 6.3) mm (Table 2). This distance increased significantly when the CC method was performed at higher positions on the tibial plafond ($P < .001$), with post hoc tests showing significant differences among all heights (Table 2).

The comparison of the CC axes of different heights showed an external rotation of 3.2 to 4.2 degrees with each increase in height (Table 3). Similarly, for each increase in height, the TS axis was also externally rotated by 6.1 to 12.6 degrees.

The inter-axis angle and distance were 8.6 (standard deviation, 4.2) degrees and 7.7 (standard deviation, 4.0) mm in the ankles with the anteverted incisurae, which were significantly smaller than in those with the retroverted incisurae (Table 4, $P < .001$ for the inter-axis angle and $P < .001$ for the inter-axis distance). There were no differences in the image measurements between the deep and shallow incisurae (Table 4).

For the intra-rater measurements, the mean difference of the inter-axis angle was 0 degrees (95% confidence interval, 0.43 degrees and -0.50 degrees), with the 95% limits of agreement being 4.4 degrees and -4.5 degrees (Supplement 1). The mean difference of the inter-axis distance was -0.1 mm (95% confidence interval, 0.32 mm and -0.53 mm), with the 95% limits of agreement being 3.9 mm and -4.1 mm. For the inter-rater measurements, systematic errors were found, with 1.8 degrees for the inter-axis angle and 1.9 mm for the inter-axis distance (Supplement 1).

DISCUSSION

This study based on CT images demonstrates that the TS axis was externally rotated relative to the CC axis, with the intersection point of the TS axis anterior to that of the CC axis. The inter-axes difference was found to be greater when the CC method was applied at a greater distance from the tibial plafond. These findings may assist surgeons in more accurately placing syndesmotic clamps and subsequent fixation along the TS axis for optimal results.

This study found that the TS axis was externally rotated relative to the

CC axis, with an overall inter-axes angle of 8.5 degrees. While the original description of the CC method indicated that the CC axis passes through the central anatomical axis, this study did not specify the axis.[4] A recent CT-based study demonstrated that the CC axis aligned almost perfectly with the axis connecting the centers of the fibula and tibia, with a difference of 0.4 degrees.[11] However, it is unclear whether clamping along the centroid axis can prevent iatrogenic syndesmotic malreduction. Another cadaveric study suggested that clamping along the TS axis or the axis internally rotated 10 degrees to the TS axis was the safe zone with the lowest malreduction rate.[7] Therefore, the CC technique provides help with determining the direction of force clamp to minimize the risk of iatrogenic syndesmotic malreduction, as long as some adjustment is made.

Our study found that the inter-axes angle increased with the height of the CC method, and the inter-axes distance also increased accordingly. These results are consistent with the finding that both the TS and CC axes externally rotated as they moved proximally, but the TS axis had a greater amount of rotation. This can be explained by the anatomy of the syndesmosis (Figure 4). When the height of the tibial plafond increased, the distal tibiofibular joint and corresponding TS axis externally rotated, while the intersection point with the medial tibial cortex moved anteriorly. Contrastingly, the anteroposterior position of the fibula relative to the tibia remained relatively stable across different heights. Consequently, external rotation of the CC axis was smaller than that of the TS axis, which agreed with a CT-based simulation study.[11] Our results are also consistent with a cadaveric study that showed the ideal medial tine of the syndesmotic clamp moved anteriorly as the height of the clamp increased from 1 to 2 cm from the plafond.[18] Based on these findings, the CC method should be applied close to the ankle joint if surgeons need to clamp the syndesmosis along the TS axis.

We found that the inter-axis angle and distance were smaller in the anteverted incisurae than in the retroverted incisurae defined as anteverted with a rotational angle of 8 degrees or higher and retroverted with a rotational angle less than 8 degrees.[3] Anteverted and shallow incisurae have been associated with an increased risk of anterior malposition of the fibula, while retroverted incisurae are associated with posterior malposition.[2, 3, 5] Taking these studies and our results together, the CC method could be applied differently depending on the syndesmotic anatomy. In the anteverted syndesmosis, clamping along the CC axis, which is slightly internally rotated to the TS axis, would be safe to push the fibula posteriorly and avoid anterior malposition of the fibula. In the retroverted syndesmosis, the clamp should be positioned along an externally rotated axis to the CC axis to push the fibula anteriorly and prevent posterior malposition. Therefore, the syndesmotic anatomy should be considered when using the CC method to reduce the syndesmosis.

In this study, inter-axis angles were examined in relation to the height from the tibial plafond and syndesmotic anatomy. However, other factors, such as the method of syndesmotic fixation (screw or suture button), also affect the quality of syndesmotic reduction. Additionally, the ideal clamp height may be dependent not only on the inter-axis angle but also on the incisura depth; the clamp should be applied where the incisura is deepest and thus stable. In this study, the incisurae were deepest at 10 mm and shallowest at 20 mm (Supplement 2). Therefore, clamping at a higher and unstable level, such as 20 mm, should be avoided to prevent iatrogenic anterior malreduction. Further research is warranted to clarify the method to obtain the optimal syndesmotic reduction.

While we evaluated the validity of the fluoroscopic CC method using the TS axis as a reference, other fluoroscopic techniques for estimating the TS axis have also been explored. The TS axis has been described as externally rotated 22 degrees from the plane of the talar dome lateral fluoroscopic view, with a narrow standard deviation of 3 degrees.[7] The axis connecting the bimalleolar tips can be used as the reference on fluoroscopy, with a difference of 4 degrees from the TS axis.[15] Another CT-based study reported that the medial position of the reduction clamp fell within the anterior third of the tibia on the lateral fluoroscopic view in 93 percent of the cases.[18] Furthermore, this fluoroscopic technique produced a malreduction rate of 0% in a clinical study.[6] Comparing our results with these studies, the tibial anterior-posterior center in the internally rotated lateral view, used in the CC method, would correspond to the tibial anterior third in the talar dome lateral view. Further research is required to determine the most effective fluoroscopic technique for reproducing the TS axis.

The present study had several limitations. First, it used digitally reconstructed radiography, which may not have accurately recreated intraoperative fluoroscopy. Although digitally reconstructed radiography has been widely used to simulate fluoroscopy and its validity against clinical fluoroscopy has been confirmed,[22] the results of this study may still represent the best-case scenario. Second, the study only included patients with foot and ankle diseases, and we carefully excluded those with ankle deformities or osteoarthritic changes, although the contralateral ankles of patients with syndesmotic injuries were ideal. Third, this was a simulation study that used CT images, so further research is required to determine whether the CC view can be reliably obtained during intraoperative fluoroscopy. Finally, different TS axis as the reference depending on the various height, similar to the previous study.[11] However, the optimal orientation for clamp application may be constant independent of the height. Further research is required to address this issue.

In conclusion, the TS axis was externally rotated to the CC axis, and the angle difference between the axes was greater when the CC method was performed higher than the tibial plafond. If surgeons aim to clamp the syndesmosis along the TS axis, the CC method should be applied closer to the ankle joint. The forceps could be placed slightly externally rotated to the CC axis. The forceps position may be adjusted depending on the fibular rotation. Further clinical studies are required to confirm the validity of the CC method.

REFERENCES

1. Bejarano-Pineda L, Guss D, Waryasz G, DiGiovanni CW, Kwon JY. The Syndesmosis, Part I: Anatomy, Injury Mechanism, Classification, and Diagnosis. *Orthop Clin North Am.* 2021;52(4):403-415. doi: 10.1016/j.ocl.2021.05.010.
2. Boszczyk A, Kwapisz S, Krümmel M, Grass R, Rammelt S. Correlation of Incisura Anatomy With Syndesmotic Malreduction. *Foot Ankle Int.* 2018;39(3):369-375. doi: 10.1177/1071100717744332.
3. Boszczyk A, Kwapisz S, Krümmel M, Grass R, Rammelt S. Anatomy of the tibial incisura as a risk factor for syndesmotic injury. *Foot Ankle Surg.* 2019;25(1):51-58. doi: 10.1016/j.fas.2017.08.003.
4. Cancienne JM, Yarboro S. Center-Center Syndesmosis Fixation Technique. *Tech Foot Ankle Surg.* 2015;14(3):134-138
5. Cherney SM, Spraggs-Hughes AG, McAndrew CM, Ricci WM, Gardner MJ. Incisura Morphology as a Risk Factor for Syndesmotic Malreduction. *Foot Ankle Int.* 2016;37(7):748-54. doi: 10.1177/1071100716637709.
6. Cosgrove CT, Putnam SM, Cherney SM, et al. Medial Clamp Tine Positioning Affects Ankle Syndesmosis Malreduction. *J Orthop Trauma.* 2017;31(8):440-446. doi: 10.1097/BOT.0000000000000882.
7. Cosgrove CT, Spraggs-Hughes AG, Putnam SM, et al. A Novel Indirect Reduction Technique in Ankle Syndesmotic Injuries: A Cadaveric Study. *J Orthop Trauma.* 2018;32(7):361-367.

doi: 10.1097/BOT.0000000000001169.

8. Gardner MJ, Demetrakopoulos D, Briggs SM, Helfet DL, Lorich DG. Malreduction of the tibiofibular syndesmosis in ankle fractures. *Foot Ankle Int.* 2006;27(10):788-92. doi: 10.1177/107110070602701005.

9. Giavarina D. Understanding Bland Altman analysis. *Biochem Med.* 2015;25(2):141-51. doi: 10.11613/BM.2015.015.

10. Harris MC, Lause G, Unangst A, et al. Prospective Results of the Modified Glide Path Technique for Improved Syndesmotic Reduction During Ankle Fracture Fixation. *Foot Ankle Int.* 2022;43(7):923-927. doi: 10.1177/10711007221081868.

11. Haupt ET, Monir JG, Mansfield M, Pollizzi A, Nichols JA, Reb CW. Computed Tomographic Validation of the Center-Center Radiographic Technique for Syndesmosis Fixation Axis Alignment in Normal Ankles. *Foot Ankle Int.* 2020;41(9):1143-1148. doi: 10.1177/1071100720936215.

12. Heifner JJ, Kilgore JE, Nichols JA, Reb CW. Syndesmosis Injury Contributes a Large Negative Effect on Clinical Outcomes: A Systematic Review. *Foot Ankle Spec.* 2022:19386400211067865. doi: 10.1177/19386400211067865.

13. Hermans JJ, Beumer A, de Jong TA, Kleinrensink GJ. Anatomy of the distal tibiofibular syndesmosis in adults: a pictorial essay with a multimodality approach. *J Anat.* 2010;217(6):633-45.

doi: 10.1111/j.1469-7580.2010.01302.x.

14. Kimura S, Yamaguchi S, Ono Y, et al. Changes in the Syndesmotic Reduction After Syndesmotic Suture-Button Fixation for Ankle Malleolar Fractures: 1-Year Longitudinal Evaluations Using Computed Tomography. *Foot Ankle Int.* 2021:10711007211008518. doi: 10.1177/10711007211008518.

15. Kumar A, Passey J, Goel L, et al. New landmarks for ideal positioning of syndesmotic screw: a computerised tomography based analysis and radiographic simulation. *Int Orthop.* 2020;44(4):665-675.
doi: 10.1007/s00264-019-04467-y.

16. Pettrone FA, Gail M, Pee D, Fitzpatrick T, Van Herpe LB. Quantitative criteria for prediction of the results after displaced fracture of the ankle. *J Bone Joint Surg Am.* 1983;65(5):667-77.

17. Phisitkul P, Ebinger T, Goetz J, Vaseenon T, Marsh JL. Forceps reduction of the syndesmosis in rotational ankle fractures: a cadaveric study. *J Bone Joint Surg Am.* 2012;94(24):2256-61.
doi: 10.2106/JBJS.K.01726.

18. Putnam SM, Linn MS, Spraggs-Hughes A, McAndrew CM, Ricci WM, Gardner MJ. Simulating clamp placement across the trans-syndesmotic angle of the ankle to minimize malreduction: A radiological study. *Injury.* 2017;48(3):770-775.
doi: 10.1016/j.injury.2017.01.029.

19. Reb CW, Brandão RA, Watson BC, Van Dyke B, Berlet GC, Prissel

MA. Medial Structure Injury During Suture Button Insertion Using the Center-Center Technique for Syndesmotic Stabilization. *Foot Ankle Int.* 2018;39(8):984-989.
doi: 10.1177/1071100718770200.

20. Rushing CJ, Spinner SM, Armstrong AV. Does Proximal Placement of the Syndesmotic Reduction Clamp Affect the Optimal Position for the Medial Tine? A Cadaveric Pilot Study. *J Foot Ankle Surg.* 2022;61(1):3-6.
doi: 10.1053/j.jfas.2021.04.005.

21. Summers HD, Sinclair MK, Stover MD. A reliable method for intraoperative evaluation of syndesmotic reduction. *J Orthop Trauma.* 2013;27(4):196-200.
doi: 10.1097/BOT.0b013e3182694766.

22. Tanaka Y, Takakura Y, Hayashi K, Taniguchi A, Kumai T, Sugimoto K. Low tibial osteotomy for varus-type osteoarthritis of the ankle. *J Bone Joint Surg Br.* 2006;88(7):909-13.
doi: 10.1302/0301-620X.88B7.17325.

23. Tornetta P, Axelrad TW, Sibai TA, Creevy WR. Treatment of the stress positive ligamentous SE4 ankle fracture: incidence of syndesmotic injury and clinical decision making. *J Orthop Trauma.* 2012;26(11):659-61.
doi: 10.1097/BOT.0b013e31825cf39c.

24. Vetter SY, Privalov M, Beisemann N, et al. Influence of ankle joint position on angles and distances of the ankle mortise using

intraoperative cone beam CT: A cadaveric study. *PLoS One.* 2019;14(5):e0217737.
doi: 10.1371/journal.pone.0217737.

25. Westermann RW, Rungprai C, Goetz JE, Femino J, Amendola A, Phisitkul P. The effect of suture-button fixation on simulated syndesmotic malreduction: a cadaveric study. *J Bone Joint Surg Am.* 2014;96(20):1732-8.
doi: 10.2106/JBJS.N.00198.

Figure 1. Digitally reconstructed radiography of the left ankle. (A) Three-dimensional computed tomographic image. (B) A digitally reconstructed radiograph of the talar dome lateral view. (C) An internally rotated lateral view with the center-center method applied. A black dot indicates the point that overlaps the anteroposterior centers of the tibia (white lines) and fibula (black lines) at a height of 0 mm from the tibial plafond (dotted line).

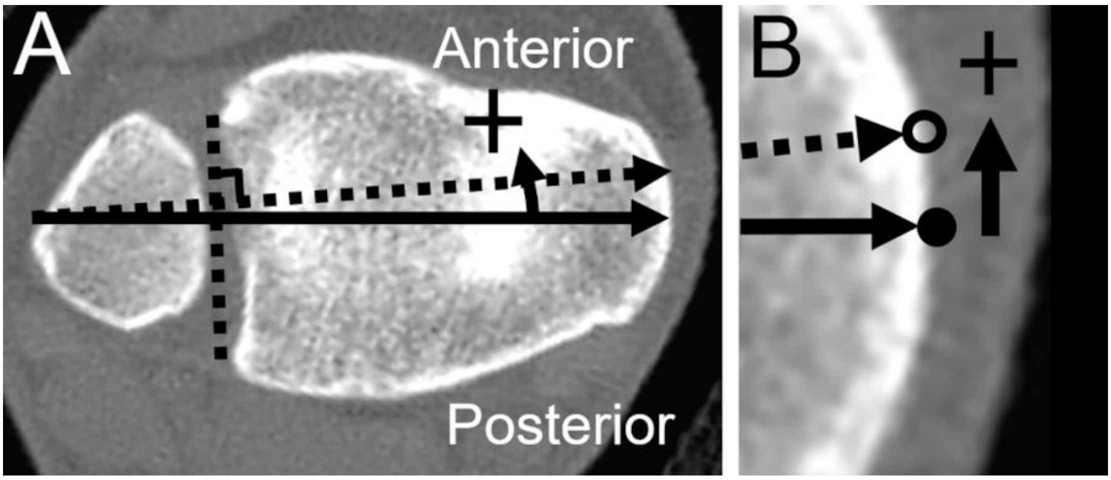

Figure 2. Computed tomography measurements taken at a height of 0 mm from the tibial plafond. (A) Inter-axes angle between the center-center axis (arrow) and trans-syndesmotic axis (dotted arrow). (B) Inter-axes distance between the intersection points of the medial tibial cortex with the center-

center (dot) and trans-syndesmotic (circle) axes.

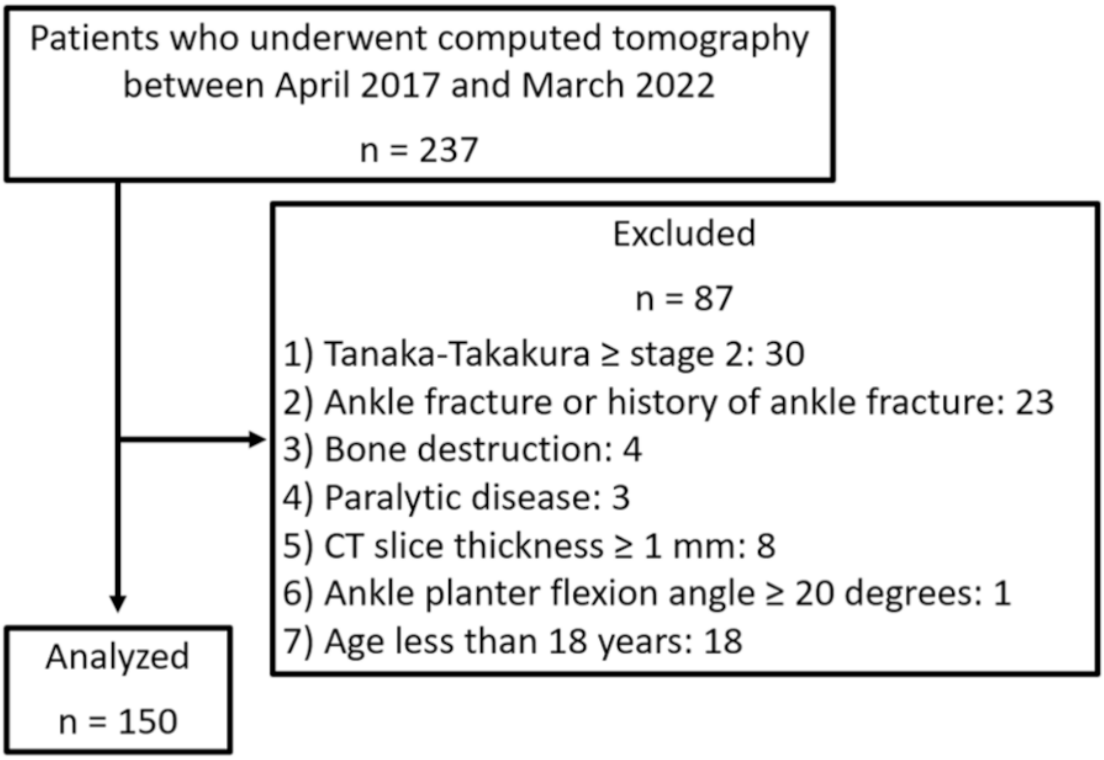

Figure 3. Flow diagram of patients.

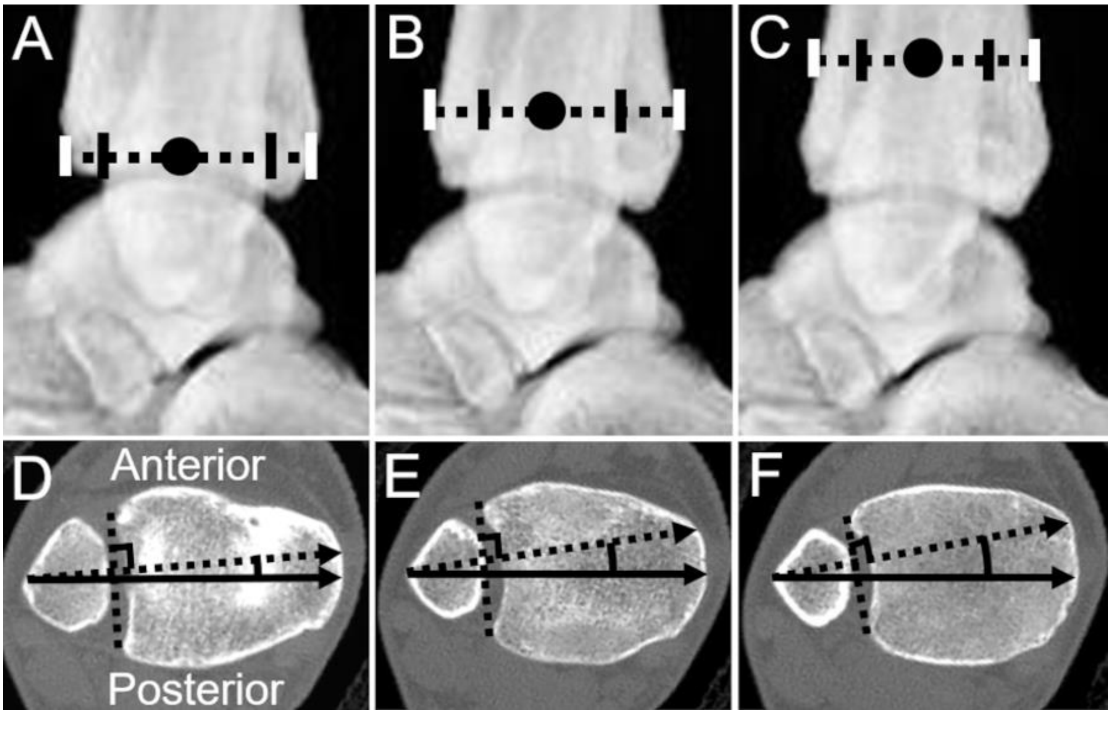

Figure 4. Center-center method of different heights from the tibial plafond and corresponding inter-axes angles on the computed tomographic images.

(A, D) 0 mm. (B, E) 10 mm. (C, F) 20 mm. The center-center (arrows) and trans-syndesmotic (dotted arrow) axes are shown.

Table 1. Patient backgrounds (n = 150).

Age (years)	51 ± 17
Gender (female / male)[a]	79 / 71
Laterality (right / left)[a]	72 / 78
Height (m)	1.6 ± 0.1
Weight (kg)	65 ± 13
Body mass index (kg/m^2)	24 ± 3.9
Diagnosis[a] (patients with the unaffected side used for analysis)	Fractures and dislocations 39 (18)
	Bone and soft tissue tumor 33
	Hallux rigidus 20
	Lisfranc joint osteoarthritis 13
	Hallux valgus 7
	Talar osteonecrosis 7 (7)
	Ankle osteoarthritis 6 (6)
	Osteomyelitis 6
	Tarsal coalition 4 (4)
	Osteochondral lesion of the talus 4
	Others 11

Values show means ± standard deviations unless indicated otherwise.

[a]Number of patients.

Table 2. Inter-axes angle and distance.

	Overall	Distance from the tibial plafond (mm)			*P*
		0	10	20	
Inter-axes angle (degrees)	8.5±6.8 (7.8–9.1)	1.9±4.0 (1.2–2.5)	10.3±5.3 (9.4–11.1)	13.2±5.1 (12.4–14.0)	< .001
Inter-axes distance (mm)	7.7±6.3 (7.1–8.3)	2.0±4.2 (1.3–2.6)	9.0±4.9 (9.0–10.5)	11.3±5.2 (10.5–12.2)	< .001

Values indicate means ± standard deviations (minimum–maximum). Horizontal bars denote significant differences in the post hoc pairwise comparisons.

Table 3. Center-center and trans-syndesmotic axes deviations between different heights from the tibial plafond.

	Distance from the tibial plafond (mm)	
	0 to 10	10 to 20
Center-center axis (degrees)	4.2±2.5 (0–12.0)	3.2±1.2 (1.0–6.0)
Trans-syndesmotic angle (degrees)	12.6±5.6 (-0.4–28.5)	6.1±5.0 (-9.4–26.5)

Values indicate means ± standard deviations (minimum–maximum).

Table 4. Inter-axes angle and distance depending on the syndesmotic anatomy at 10 mm from the tibial plafond.

	Rotation		*P*	Depth		*P*
	Anteverted (n = 89)	Retroverted (n = 61)		Deep (n = 81)	Shallow (n = 69)	
Inter-axes angle (degrees)	8.0±4.2 (-4.0–16.7)	13.6±4.8 (-1.1–24.1)	< .001	9.7±5.2 (-4.0–23.4)	10.8±5.3 (-0.8–23.4)	0.2
Inter-axes distance (mm)	7.7±4.0 (-3.4–17.3)	12.8±4.5 (-0.8–23.4)	< .001	9.4±4.9 (-3.4–23.4)	10.0±4.9 (-0.8–22.7)	0.5

Values indicate means ± standard deviations (minimum–maximum).

Supplement 1. Bland-Altman plot of measurement error. Intra-rater error for the inter-axis angle (A) and inter-axis distance (B). Inter-rater error for the inter-axis angle (C) and inter-axis distance (D).

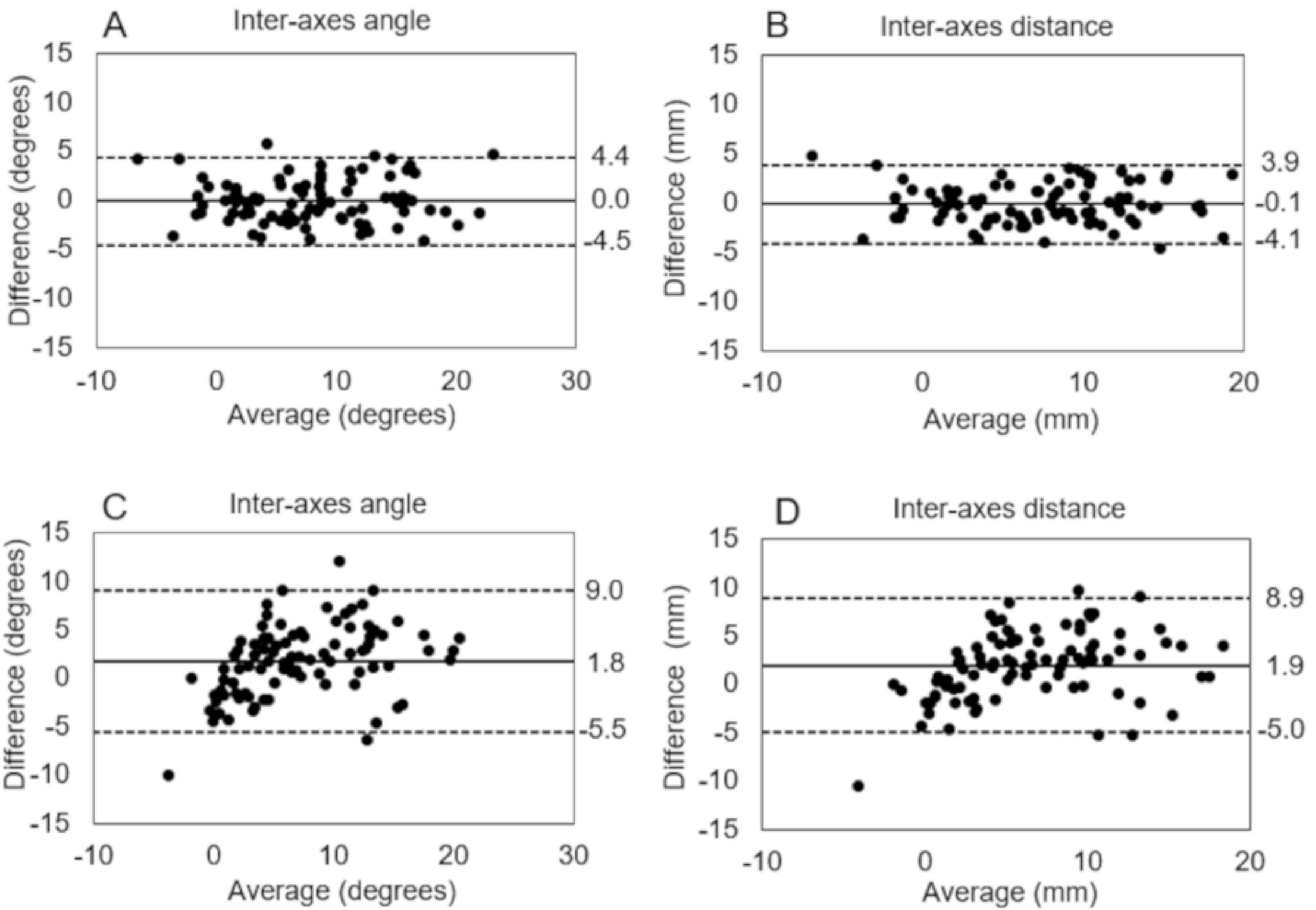
A
Inter-axes angle
Difference (degrees)
Average (degrees)
4.4
0.0
-4.5
B
Inter-axes distance
Difference (mm)
Average (mm)
3.9
-0.1
-4.1
C
Inter-axes angle
Difference (degrees)
Average (degrees)
9.0
1.8
-5.5
D
Inter-axes distance
Difference (mm)
Average (mm)
8.9
1.9
-5.0

Supplement 2. Depths of the fibular incisura at different height from the tibial plafond.

	Distance from the tibial plafond (mm)			P^a
	0	10	20	
Incisura depth (mm)	3.4 ± 1.3 (0–8.1)	3.9 ± 1.2 (0.4–7.0)	1.3 ± 0.8 (0–3.6)	< .001

Values indicate means ± standard deviations (minimum–maximum). [a]Repeated measures one-factor analysis of variance. Horizontal bars denote significant differences in the post hoc pairwise comparisons.

Foot & Ankle International　Vol.44　No.11

2023 年 9 月 26 日　公表済

DOI: 10.1177/10711007231198818.